# MULTIPLE FEATURE FUSION FOR FINE CLASSIFICATION OF CROPS IN UAV HYPERSPECTRAL IMAGERY


*Yajing Liang[1,2], Lifei Wei[1,2,3], Qikai Lu[2,3]*

1.Key Laboratory of Urban Land Resources Monitoring and Simulation，Ministry of Land and Resources, Shenzhen 518034, China;

2.Faculty of Resources and Environmental Science, Hubei University, Wuhan 430062, China;

3.Hubei Key Laboratory of Regional Development and Environmental Response, Hubei University, Wuhan 430062, China



## ABSTRACT

UAV hyperspectral imagery has been widely applied in the fine classification of crops because of its high spectral resolution and high spatial resolution. As the crops in hyperspectral image show complicated characteristics, only the spectral information is insufficient to distinguish them. Therefore, we use multiple feature fusion method for fine classification of crops in UAV hyperspectral imagery. In our work, the GLCM texture, morphological profile, and endmember abundance feature, are extracted. Meanwhile, three fusion strategies, namely decision fusion, probability fusion, and stacking fusion, are employed to obtain the classification results. The experimental results illustrate the superiority of the multiple fusion approaches in the crop fine classification with hyperspectral imagery.



***Index Terms***—UAV hyperspectral imagery, fine classification of crops, multiple feature fusion


## 1. INTRODUCTION

Agriculture is the foundation of national industry, which provides basic materials for other sectors of the national economy. Fine classification of crops can obtain information for agricultural monitoring, yield estimation, and government planning [1],[2]. With the development of remote sensing technology, UAV hyperspectral images have been widely used in agriculture [3],[4]. The UAV hyperspectral images show unlimited revisit period, high spatial resolution and high spectral resolution, which is satisfactory information source for precision agriculture.

Recently year, a lot of researchers pay attention to the fine classification of crops on UAV hyperspectral image [5]. Melgani, Liu, Zhang, *et al.* classify crops on the basis of the spectral information of hyperspectral images [6]-[8]. Tarabalka, Wang, Wu Jian, *et al.* take the spatial characteristics of the image into account to improve the classification performance [9]-[11]. However, crops show complicated characteristics in hyperspectral image, it is difficult to obtain a promising classification result with a single feature.

In this context, the multiple feature fusion strategy is employed to obtain the fine crop classification results. The spectral channels are fused with a variety of spatial features. In this work, the GLCM texture, endmember abundance features, morphological profiles are considered. Meanwhile, three strategies, including decision fusion, probability fusion, and stacking fusion, are utilized. The experiments are conducted on a UAV image obtained over an agricultural area in Honghu city.

## 2. METHOD

### 2.1. Multi-Feature extraction

*2.1.1 GLCM texture*

Gray Level Co-occurrence Matrix (GLCM) is a widely accepted textural information extraction method for remote sensing image analysis. GLCM can reflects the comprehensive information of image gray about direction, adjacent interval and change amplitude [12]. Moreover, GLCM is the basis of analyzing local patterns and their arrangement rules.

$$P(i,j,d,\theta)=\#\left\{(x_1,y_1),(x_2,y_2)\in M,N \,\middle|\, f(x_1,y_1)=i, f(x_2,y_2)=j\right\} \quad (1)$$

where $f(x,y)$ is a 2-dimensional digital image with the size of the image is set to $M \times N$. Let $\#(x)$ be the number of elements in the set x, and $Ng \times Ng$ matrix is represented by $P$. If the distance between $(x_1,y_1)$ and $(x_2,y_2)$ is $d$ and the corresponding angle is $\theta$.

*2.1.2 Morphological profiles*

Morphology profiles can extract the structural information of image [13]. Let $\gamma^{SE}(I)$ be the morphological reconstruction of opening on image $I$ with structural element $SE$. Where $\gamma^{SE}(I)$ is the morphological opening and $\varphi^{SE}(I)$ is morphological closing. A series of $SE$s of increasing size are defined as MPs:

$$\begin{aligned} \mathrm{M}P_{\gamma} &= \{MP_{\gamma}^{\lambda}(I)=\gamma^{\lambda}(I)\},\ \forall\lambda\in[0,n] \\ \mathrm{M}P_{\varphi} &= \{MP_{\varphi}^{\lambda}(I)=\varphi^{\lambda}(I)\}, \forall\lambda\in[0,n] \end{aligned} \quad (2)$$

In the formula, $\lambda$ is the radius of a disk $SE$. A series of $SEs$ with gradually increasing size are used to display the multi-scale information of the image.

*2.1.3 Endmember abundance feature*

Considering the spatial resolution of sensors, there are several mixed pixels exist in remote sensing images. Therefore, the endmember abundance is also extracted for the fine classification of crops. In this work, sequential Maximum Angle Convex Cone (SMACC) that is based on convex cone model is employed. SMACC method can extract endmember abundance images from remote sensing images.

$$H(c,i) = \sum_{k}^{N} R(c,k)A(k,j) \tag{3}$$

Where $H$ is the endmember of the spectral; the band index is $c$, and the pixel index is $i$; $k$ and $j$ express the index from 1 to the largest endmember; $R$ means the matrix containing the endmember spectral; $A$ is the abundance of the endmember $j$ to the endmember $k$ in each pixel Degree matrix [14].

## 2.2. Fusion strategy

*2.2.1 Decision fusion*

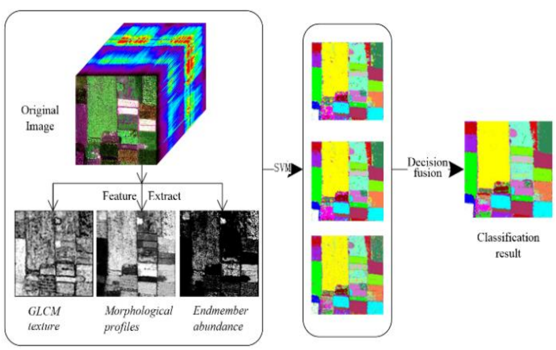


Fig. 1. Flowchart of the decision fusion strategy

Decision fusion combines the classification results obtained with different features. The extracted features are integrated with the spectral feature to achieve the initial classification results. For each pixel in the hyperspectral images, it can be assigned to different classes with different feature. The decision fusion takes the class with most frequent occurrence as the category of this pixel. Therefore, a classification map can be given on the basis of the classification results of multiple features. The flowchart of the multi-feature decision fusion strategy is shown in Fig 1.

*2.2.2 Probability fusion*

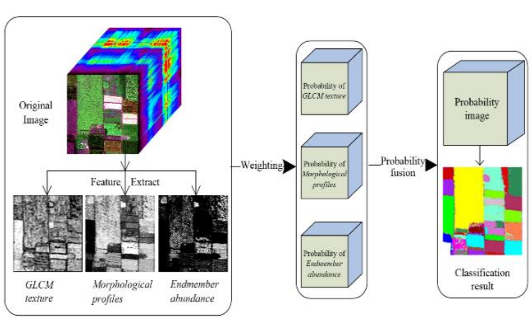


Fig. 2. Flowchart of the probability fusion strategy

Different from decision fusion strategy, probabilistic fusion is based on the probability output of the classifiers. First, we obtain the classification probability results with each group of features. By averaging the probability outputs obtained with different features, the fused probability classification results can be generated. Then, for each pixel, the class with the highest probability is selected as its label, which can be described as:

$$C(x) = argmax_{k-\{1\dots k\}}\left\{\frac{1}{F} p_f^k(x)\right\} \tag{4}$$

Where $F$ is the total number of features; $p_f^k(x)$ represents the probability value of pixel $x$ in the output result of feature $f$ corresponding to category $k$. Fig. 2. shows the flowchart of probability fusion approach.

*2.2.3 Stacking fusion*

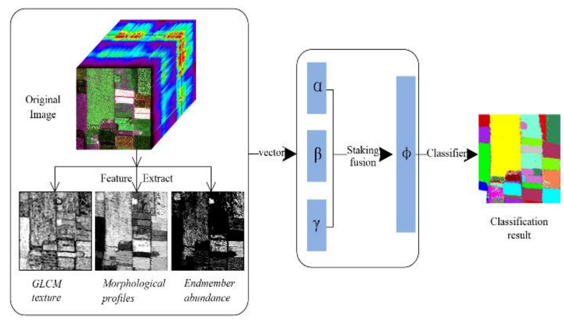


Fig. 3. Flowchart of the staking fusion strategy

Stacking fusion is the most common fusion strategy. We directly superpose the vectors of spectral features and GLCM texture, morphological profile, endmember abundance feature to generate new vectors. For each pixel in the image, the fusion feature of the pixel instead of the spectral feature is used of the classification feature, and inputs the classifier. Staking fusion as shown in Fig. 3.

$$\gamma = [\varphi_{spec}^T X_{spec}, \varphi_{spat}^T X_{spat}] \tag{5}$$

Let $X_{spec}$ be the spectral feature, $X_{spat}$ be the feature related to the extended the morphological profiles, GLCM texture, and endmember abundance features. Then, there is the feature fusion expression, where $\gamma$ is the fusion feature and $\varphi$ is the linear mapping moment of the extracted feature.

## 3.EXPERIMENTAL RESULTS

### 3.1 Data set

Honghu dataset was acquired on November 20, 2017, in Honghu City, Hubei province, China. DJI Matrice 600 Pro equipped on a 17-mm focal length Headwall Nano-Hyperspecl imaging sensor. The experimental area is a complex planting-area of crops, including pakchoi cabbage and cabbage, celtuce and film-covered lettuce. The altitude of hyperspectral image acquisition is 100 meters. The size of the hyperspectral imagery is 400 × 400 pixels, and image has 274 bands. The spatial resolution of the UAV-borne hyperspectral imagery is about 0.04m. An overview of Honghu data is shown in Fig. 4.

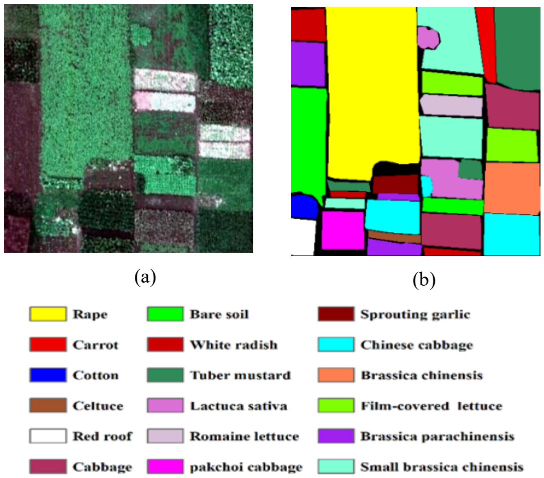


Fig. 4. Honghu: (a) the original image; (b)the ground-truth map

### 3.2 Experimental result

The Honghu data set is used to verify the method of fine classification of crops in UAV hyperspectral imagery using multiple features. We designed seven sets of experiments: Original image, GLCM texture, Endmember abundance feature, Morphological profiles, Decision fusion, Probability fusion and Stacking fusion.

To describe the textural information extracted by GLCM, we use six kinds of measurement, namely, mean, homogeneity, contrast, dissimilarity, entropy and second moment, in this work. The windows of the GLCM texture are set to 7×7. And, the four directions 0 ˚, 45 ˚, 90 ˚, 135 ˚ are utilized. Then, the GLCM texture is obtained by averaging the above four directions. The morphological profiles are obtained through morphological opening and closing reconstruction with disk-shaped *SE*. The radius of *SE* is set to 1, 3, 5, and 7. Endmember abundance feature is obtained by SMACC. Among them, the number of extracted endmembers is 4, and RMS Error Tolerance is set to 0. Additionally, the base image for GLCM texture and morphological profiles extraction is the first 8 principal components that are obtained by using principal component analysis.

Support vector machine (SVM) is used as the classifier to obtain classification results. The radial basis function is used, Gamma in kernel function is set to 1, the penalty parameter is set to 100. 3% of ground-truth samples are randomly selected and used as the training set. And the rest 97% samples are employed for testing. The Overall Accuracy (OA), KAPPA coefficient, and accuracy of each category are used to evaluate the classification performance.

The classification results are shown in Fig.5, and the accuracies are reported in Table 1. Fig.5. (a) is the classification results with spectral properties, and the OA reaches 81%. Additionally, the accuracies of pakchoi cabbage, romaine lettuce and carrot are all below 50%. Fig.5. (b), (c), (d) are the classification results with GLCM texture, endmember abundance feature, and morphological profiles, respectively. Fig.5. (b) and (d) are better than the spectral-based result, but there are still several noises and misclassified pixels. Compared to the spectral-based method, the OAs of GLCM texture and morphological profiles are increased by 7% and 10%, respectively. But the result of endmember abundance feature is unsatisfactory.

The results of decision fusion and probability fusion are shown in Fig.5. (e), (f). The misclassification phenomenon is significantly reduced, and OA is above

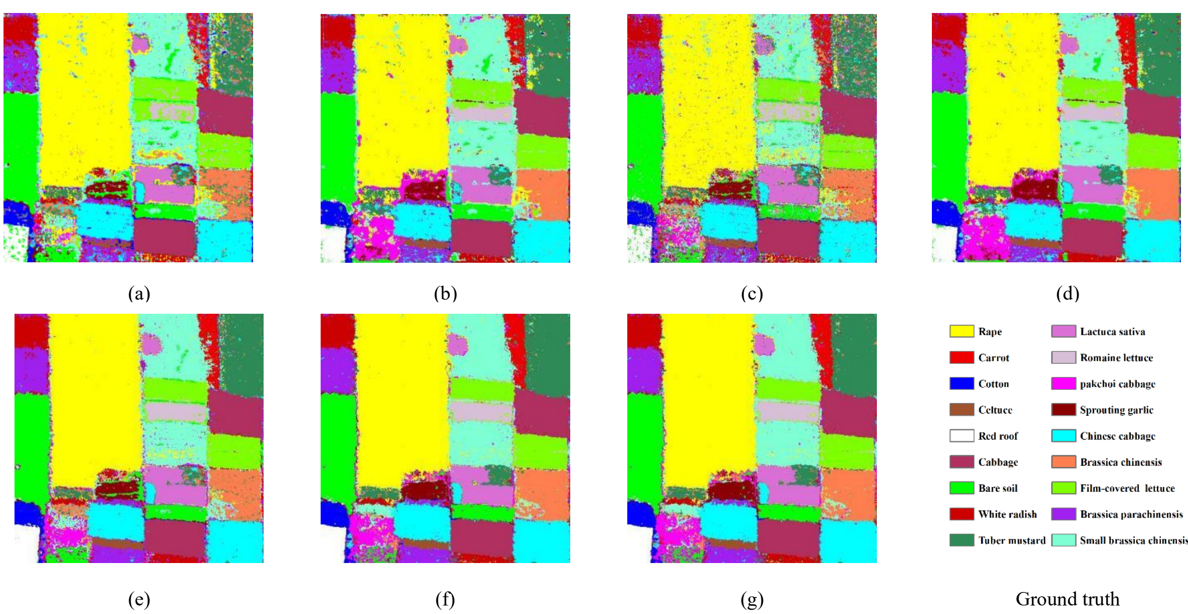


Fig.5. Classification results: (a) Original Spectral, (b) GLCM Texture, (c) Endmember Abundance, (d) Morphological Profiles, (e) Decision Fusion, (f) Probability Fusion, and (g) Stacking Fusion.

Table 1. Honghu data classification results

| Types | Training Samples | Text Samples | Original Spectral | GLCM Texture | Endmember Abundance | Morphological Profiles | Decision Fusion | Probability Fusion | Stacking Fusion |
|---|---|---|---|---|---|---|---|---|---|
| Red roof | 66 | 2138 | 81.06 | 95.37 | 75.02 | 99.86 | 96.18 | 99.34 | 99.53 |
| Bare soil | 354 | 11456 | 94.93 | 96.67 | 93.92 | 96.84 | 94.73 | 95.45 | 98.60 |
| Cotton | 42 | 1382 | 79.45 | 92.62 | 78.65 | 95.42 | 90.39 | 97.50 | 98.19 |
| Rape | 1137 | 36783 | 95.88 | 96.58 | 95.81 | 98.36 | 94.78 | 98.65 | 99.08 |
| Chinese cabbage | 323 | 10472 | 92.42 | 93.91 | 91.23 | 96.57 | 89.74 | 96.74 | 98.02 |
| Pakchoi cabbage | 121 | 3934 | 14.69 | 69.06 | 12.25 | 51.83 | 74.85 | 62.47 | 68.51 |
| Cabbage | 309 | 9998 | 97.65 | 99.00 | 97.15 | 98.41 | 88.45 | 91.01 | 99.55 |
| Tuber mustard | 343 | 11098 | 62.52 | 81.32 | 61.09 | 86.61 | 81.90 | 90.07 | 93.81 |
| Brassica parachinensis | 189 | 6114 | 73.37 | 79.78 | 70.46 | 90.13 | 85.73 | 95.82 | 89.12 |
| Brassica chinensis | 217 | 7036 | 56.38 | 75.20 | 53.47 | 73.94 | 81.21 | 76.58 | 85.66 |
| Small brassica chinensis | 477 | 15451 | 80.51 | 86.87 | 79.46 | 88.29 | 83.26 | 89.91 | 95.05 |
| Lactuca sativa | 158 | 5114 | 77.53 | 84.53 | 76.42 | 89.88 | 85.61 | 92.31 | 92.02 |
| Celtuce | 30 | 973 | 55.60 | 76.57 | 46.35 | 93.49 | 86.57 | 92.80 | 89.83 |
| Film-covered lettuce | 217 | 7046 | 89.11 | 94.86 | 88.08 | 96.54 | 92.62 | 96.70 | 96.74 |
| Romaine lettuce | 90 | 2921 | 46.73 | 71.59 | 46.18 | 86.89 | 87.09 | 88.38 | 90.28 |
| Carrot | 83 | 2710 | 46.83 | 65.46 | 46.01 | 77.20 | 85.08 | 83.57 | 87.90 |
| White radish | 122 | 3960 | 69.70 | 72.65 | 67.47 | 88.76 | 86.53 | 90.88 | 89.47 |
| Sprouting garlic | 61 | 2005 | 60.25 | 74.81 | 56.21 | 74.78 | 88.79 | 85.05 | 88.63 |
| OA | | | 81.24% | 88.89% | 80.04% | 91.50% | 92.36% | 92.98% | 94.92% |
| Kappa | | | 0.7866 | 0.8741 | 0.7729 | 0.9037 | 0.9108 | 0.9206 | 0.9425 |

92%. Fig.3. (g) shows the result of stacking fusion. Compared with the results of decision fusion and probability fusion, the classification performance is significantly improved. The OA of stacking fusion reaches 94.9%, and the highest class-specific accuracy is 99.55%. Experiments prove that the multiple feature fusion method can obtain good results.

## 4.CONCLUSION

In this paper, we proposed a multiple feature fusion method for fine classification of crops in UAV hyperspectral images. The experiments conducted on the Honghu Dataset prove the feasibility of the multiple feature fusion method, and the feature stacking approach give the best result. The fusion of multiple features can improve classification accuracy and reduce noise and misclassification. In the future, more state-of-the-art classifier will be taken into account.

## REFERENCES


[1] Konstantinos Makantasis, Konstantinos Karantzalos, Anastasios Doulamis, Nikolaos Doulamis. Deep supervised learning for hyperspectral data classification through convolutional neural networks. IEEE International Geoscience and Remote Sensing Symposium (IGARSS), 2015:4959 – 4962.

[2] RAO N.R.. Development of a crop-specific library and discrimination of various agricultural crop varieties using hyperspectral imagery. International Journal of Remote Sensing,2008,29(1):131~144.

[3] Youngsinn S., Sanjay R.N.. Supervised and unsupervised spectral angle classifiers. Photogrammetric Engineering and Remote Sensing,2002,68 (12):1271~1280.

[4] Chen C., Li W., Su H.J., *et al.* Spectral-spatial classification of hyperspectral image based on kernel extreme learning machine. Remote Sensing,2014(6):5795~5814.

[5] Li F., Wang J., Lan R.S., *et al*. Hyperspectral image classification using multi-feature fusion. Optics and Laser Technology,2019 (110):176~183.

[6] Melgani F, Bruzzone L. Classification of hyperspectral remote sensing images with support vector machines[J]. IEEE Transactions on Geoscience and Remote Sensing, 2004, 42(8):1778-1790.

[7] Liu Liang, Jiang Xiaoguang, Li Xianbin, Tang Lingli. Study on Crop Classification Methods Using Hyperspectral Remote Sensing Data[J]. Journal of the Graduate School of the Chinese Academy of Sciences,2006(04):484-488.

[8] Zhang Yue, Guan Yunlan. Hyperspectral Band Reduction by Combining Clustering with Adaptive Band Selection [J]. Remote Sensing Information, 2018, 33(02): 66-70.

[9] Tarabalka Y, Fauvel M, Chanussot J, *et al*. SVM and MRF-Based Method for Accurate Classification of Hyperspectral Images[J]. IEEE Geoscience & Remote Sensing Letters, 2010, 7(4):736-740.

[10] WANG Zeng-mao, DU Bo, ZHANG Liang-pei, ZHANG Le-fei. Based on Texture Feature and Extend Morphological Profile Fusion for Hyperspectral Image Classification[J]. ACTA PHOTONICA SINICA, 2014, 43(8): 0810002

[11] Wu Jian, Peng Daoli. Vegetation classification technology of hyperspectral remote sensing based on spatial information [J]. Journal of agricultural engineering, 2012,28 (05): 150-153

[12] R. M. Haralick, K. Shanmugam and I. Dinstein, "Textural Features for Image Classification," in IEEE Transactions on Systems, Man, and Cybernetics, vol. SMC-3, no. 6, pp. 610-621, Nov. 1973, doi: 10.1109/TSMC.1973.4309314.

[13] Hu Xuan, Lu Qikai. Hyperspectral Image Classification Algorithm Based on Saliency Profile[J]. Acta Optica Sinica, 2020, 40(16): 1611001.

[14] Gao Xiaohui, Xiang Libin, Wei Ruyi, LV qunbo, Wei Junxia. Research on Endmember Extraction Algorithm Based on Spectral Classification [J]. Spectroscopy and spectral analysis, 2011,31 (07): 1995-1998